Supplementary Information

Title: Global estimates of ambient reactive nitrogen components during 2000-2100 based on the multi-stage model

Authors: Rui Li[a, b *], Yining Gao[a], Lijia Zhang[a], Yubing Shen[a], Gehui Wang[a]

Affiliations: [a] *Key Laboratory of Geographic Information Science of the Ministry of Education, School of Geographic Sciences, East China Normal University, Shanghai, 200241, PR China*

[b] *Institute of Eco-Chongming (IEC), 20 Cuiniao Road, Chenjia Town, Chongming District, Shanghai, 202162, China*

*** Corresponding author**

Prof. Li (rli@geo.ecnu.edu.cn)

Number of pages: 18

Number of figures: 16

Number of tables: 1

Table S1 The basic information and data sources of variables for N-bearing component estimates.

Dataset	Variable	Unit	Spatial resolution	Time resolution	Data source
N-bearing components	NO_3^-	$\mu g/m^3$	--	Monthly	NNDMN, EANET, EMEP, and CASTNET
	HNO_3	$\mu g/m^3$	--	Monthly	
	NH_3	$\mu g/m^3$	--	Monthly	
	NH_4^+	$\mu g/m^3$	--	Monthly	
NO_2 tropospheric column	NO_2 column	$mole/cm^2$	0.25°	Daily	NASA
NH_3 column	NH_3 column	mol/cm^2	0.5°	Daily	ISAI
Meteorology	D_{2m}	℃	0.25°	6-hour	ERA-Interim reanalysis product
	T_{2m}	℃	0.25°	6-hour	
	U_{10}	m/s	0.25°	6-hour	
	V_{10}	m/s	0.25°	6-hour	
	BLH	m	0.25°	3-hour	
	Sund	s	0.25°	6-hour	
	Sp	hPa	0.25°	6-hour	
	Tp	mm	0.25°	6-hour	
Land use types	Barren land	m^2	30 m	Annually	Liu et al. (2020)
	Grassland	m^2	30 m	Annually	
	Shrubland	m^2	30 m	Annually	
	Forest	m^2	30 m	Annually	
	Cropland	m^2	30 m	Annually	
	Tundra	m^2	30 m	Annually	
	Snow/ice	m^2	30 m	Annually	
Elevation	DEM	m	30 m	--	ETOPO

Table S2 Available (O) and not available (X) CMIP6 Global Climate Models used in our study.

	SSP1-2.6	SSP2-4.5	SSP3-7.0	SSP8.5
ACCESS-ESM1-5	O	O	O	O
CanESM5	O	O	O	O
CESM2-WACCM	O	O	O	O
CMCC-CM2-SR5	O	O	O	O
EC-Earth3-Veg	O	O	O	O
EC-Earth3-CC	X	O	X	O
FGOALS-f3-L	O	O	O	O
FGOALS-g	O	O	O	O
GFDL-ESM4	O	O	O	O
INM-CM5-0	O	O	O	O
IPSL-CM6A-LR	O	X	X	X
MIROC6	O	O	O	O
MPI-ESM1-2-HR	O	O	O	O
MRI-ESM2-0	O	O	O	O
Nor-ESM2-LM	O	O	O	O
NorESM2-MM	O	O	O	O

Figure S1 The spatial distribution of monitoring sites of reactive nitrogen components at the global scale. The color bar reflects the map of global terrain (altitude).

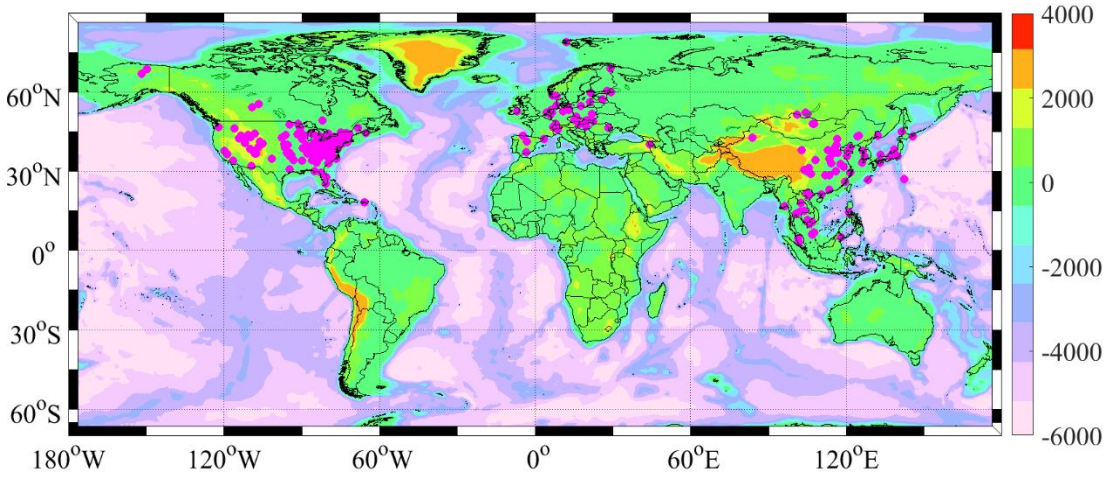

Figure S2 The predictive performances of four N-bearing components including NO_3^- (a), HNO_3 (b), NH_3 (c), and NH_4^+ (d) based on ensemble model. The model was constructed with 90% original data and the remained data was applied to validate the model. The black solid line denotes the best-fitting curve for all of the points, while the black dashed line represents the diagonal, which means the same observed and simulated values.

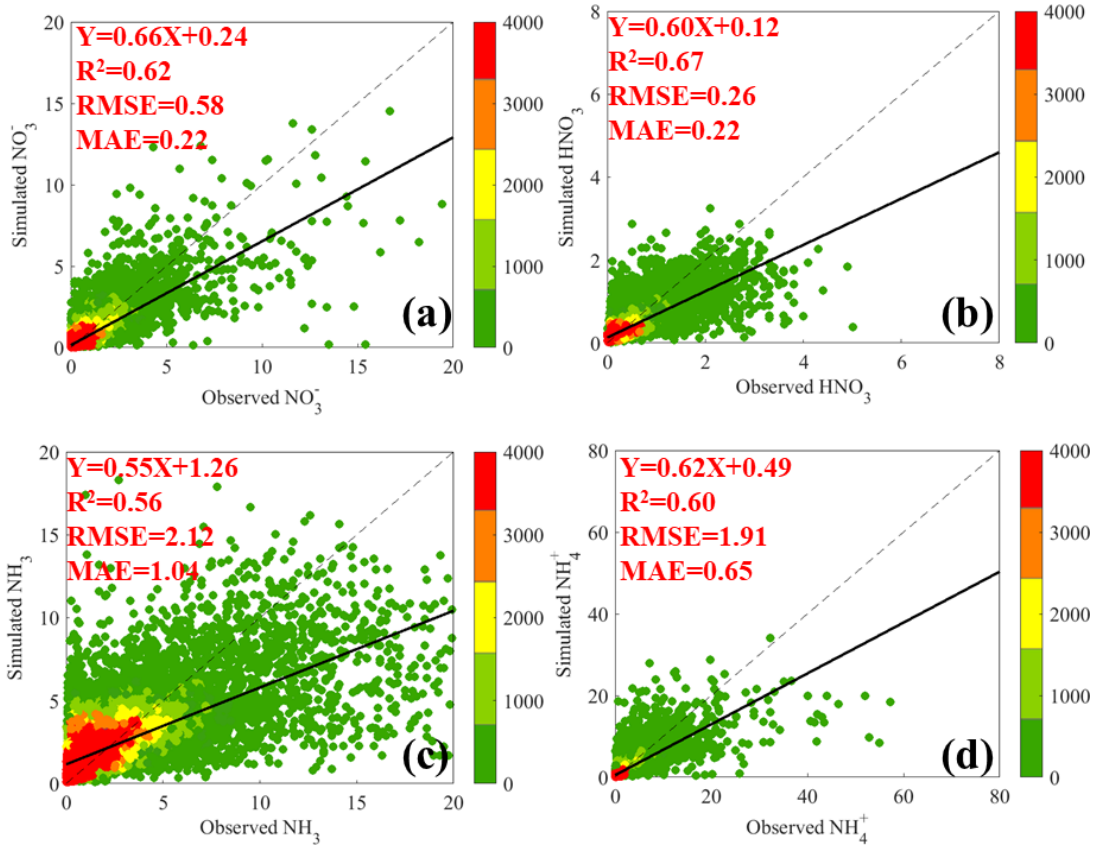

Figure S3 The annual mean concentrations of NO_3^- (a), HNO_3 (b), NH_3 (c), and NH_4^+ (d) at the global scale (Unit: μg N m^{-3}).

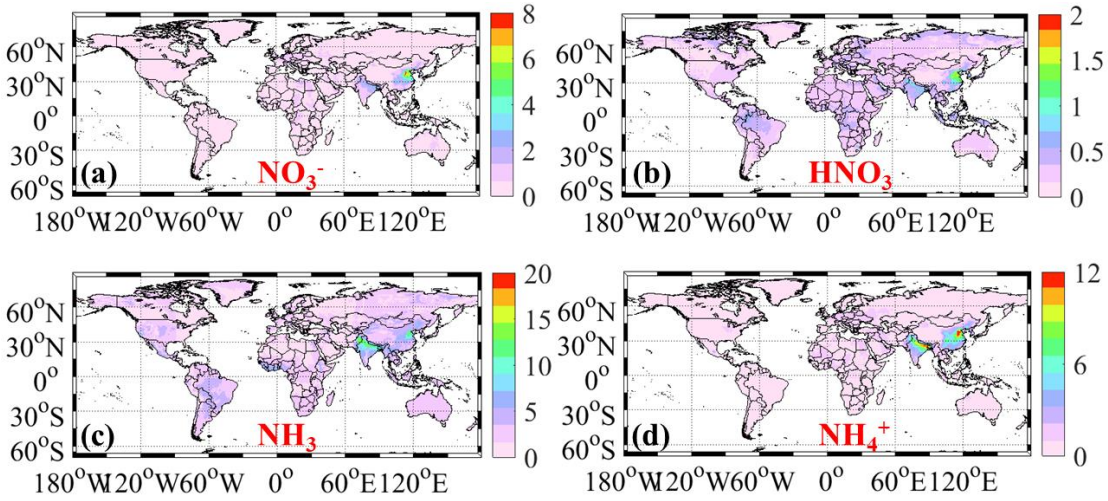

Figure S4 The seasonal variations of NO_3^- levels at the global scale (Unit: μg N m^{-3}).

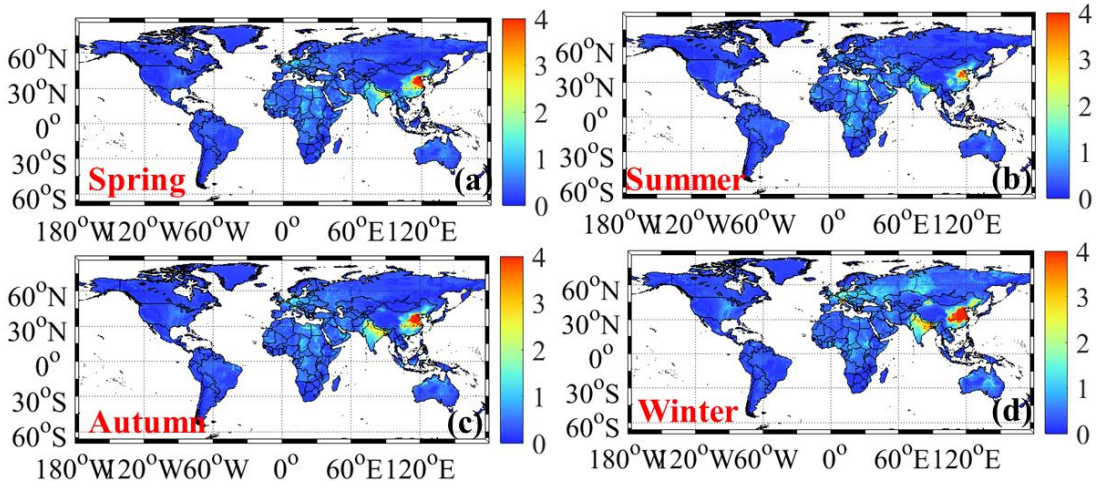

Figure S5 The seasonal variations of HNO_3 levels at the global scale (Unit: μg N m^{-3}).

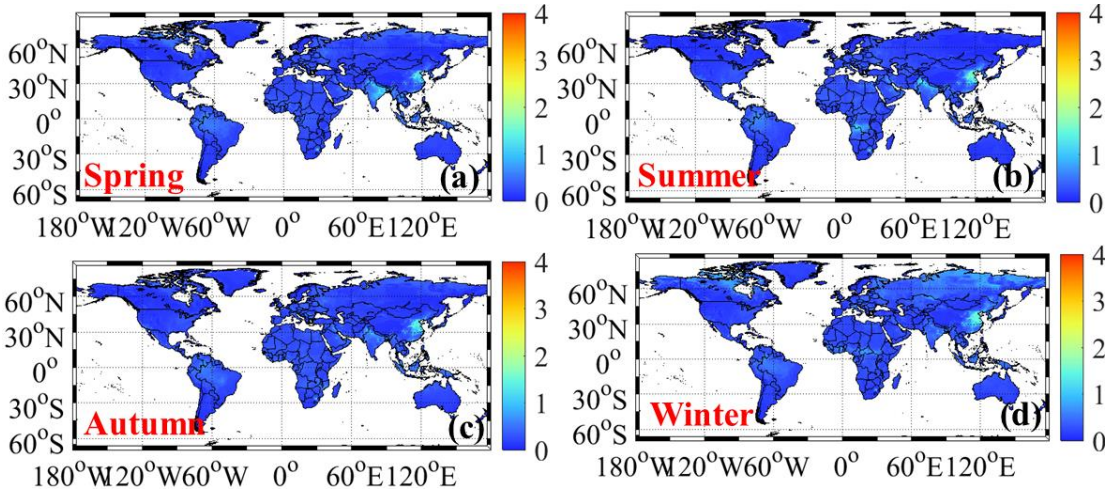

Figure S6 The seasonal variations of NH_3 levels at the global scale (Unit: μg N m^{-3}).

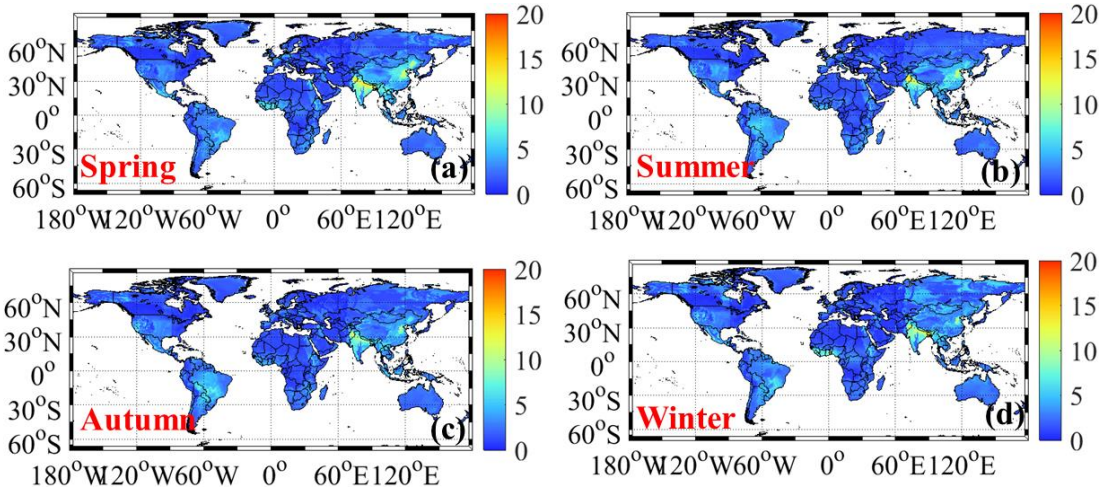

Figure S7 The seasonal variations of NH_4^+ levels at the global scale (Unit: μg N m^{-3}).

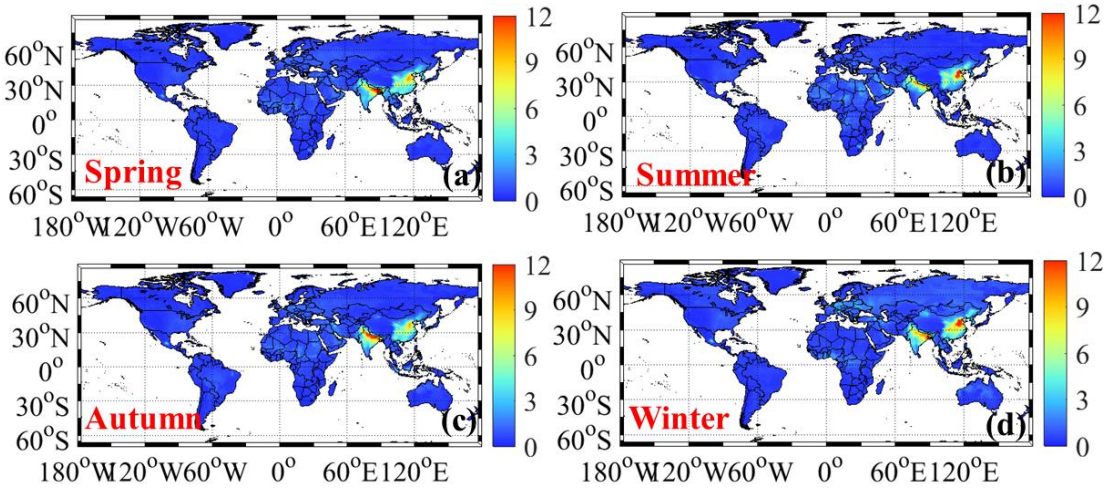

Figure S8 The monthly variations of NO_3^-, HNO_3, NH_3, and NH_4^+ in China, Europe, and the United States (Unit: μg N m^{-3})

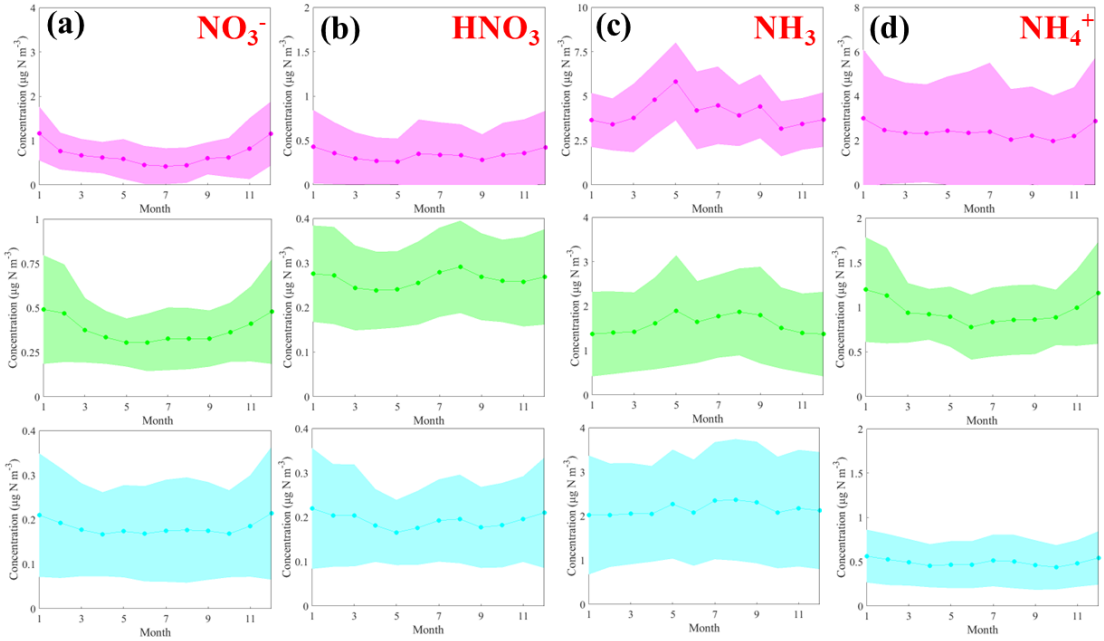

Figure S9 The yearly variations of NO_3^- (a), HNO_3 (b), NH_3 (c), and NH_4^+ (d) concentrations around the world during 2000-2019 (Unit: μg N m^{-3}/yr).

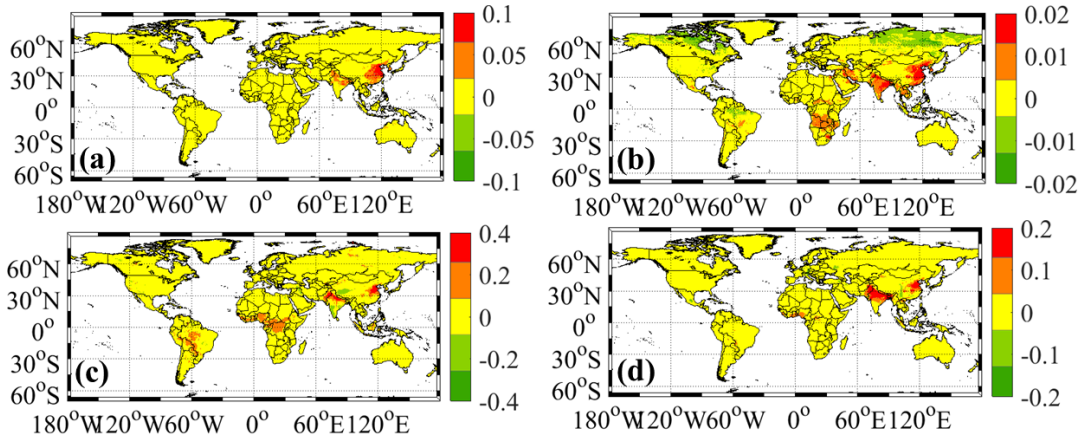

Figure S10 The yearly variations of NO_3^- (a), HNO_3 (b), NH_3 (c), and NH_4^+ (d) concentrations around the world during 2000-2007 (Unit: μg N m^{-3}/yr).

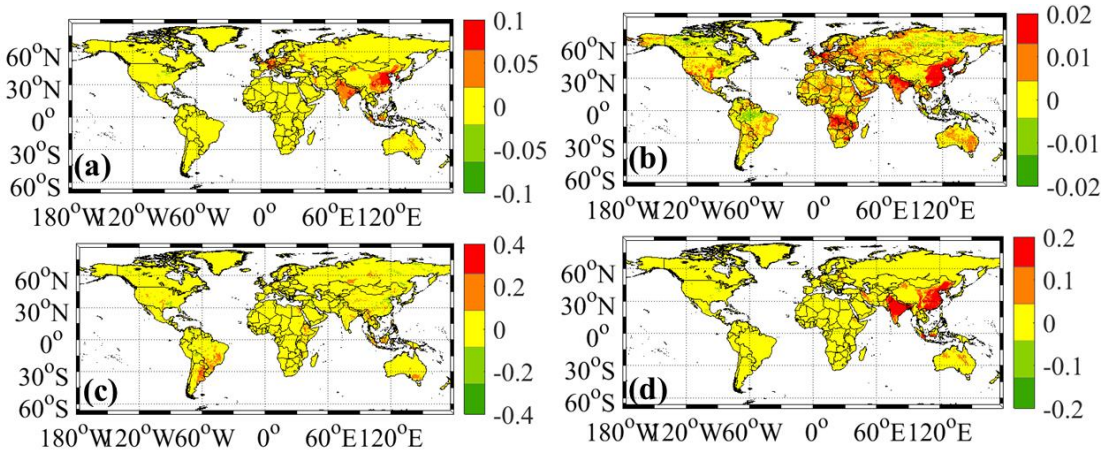

Figure S11 The yearly variations of NO_3^- (a), HNO_3 (b), NH_3 (c), and NH_4^+ (d) concentrations around the world during 2007-2013 (Unit: μg N m^{-3}/yr).

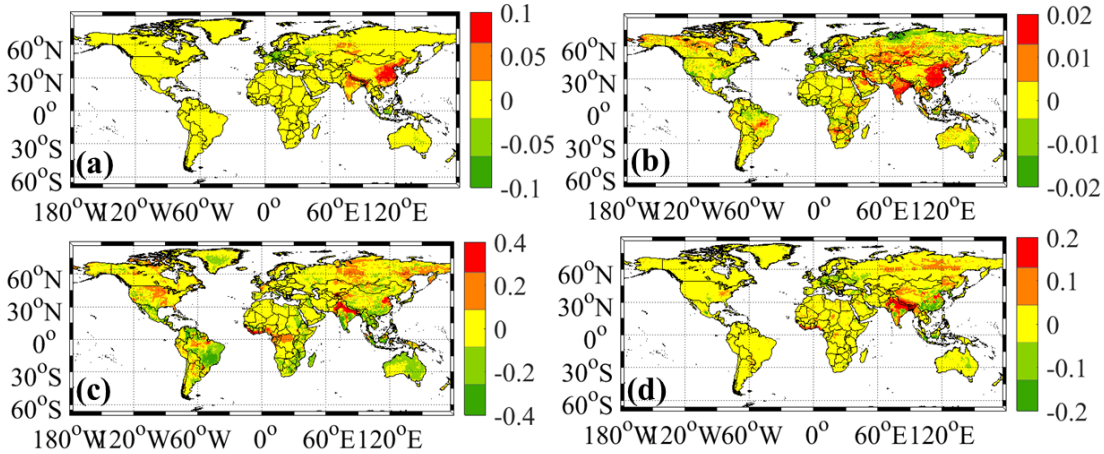

Figure S12 The yearly variations of NO_3^- (a), HNO_3 (b), NH_3 (c), and NH_4^+ (d) concentrations around the world during 2013-2019 (Unit: μg N m^{-3}/yr).

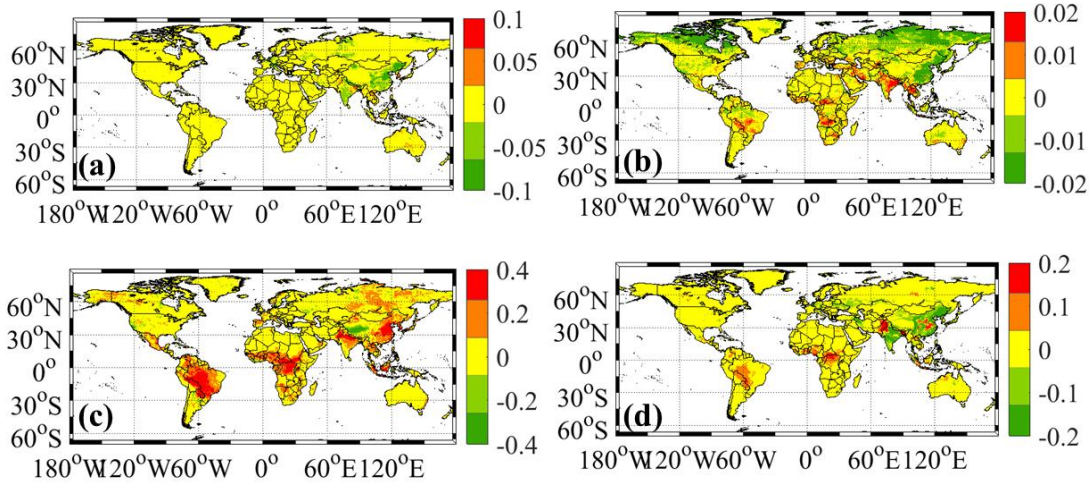

Figure S13 Spatial variations of projected global ambient NO_3^- concentrations under different climate change scenarios (Unit: μg N m^{-3}). Panels (a-d) represent the annual mean concentrations of NO_3^- concentrations for 2030s (2021-2050 average), 2050s (2041-2070 average), 2070s (2061-2090 average), and 2080s (2071-2100 average) under SSP1-2.6 scenarios. Panels (e-h) represent the annual mean concentrations of NO_3^- concentrations for 2030s (2021-2050 average), 2050s (2041-2070 average), 2070s (2061-2090 average), and 2080s (2071-2100 average) under SSP2-4.5 scenarios. Panels (i-l) represent the annual mean concentrations of NO_3^- concentrations for 2030s (2021-2050 average), 2050s (2041-2070 average), 2070s (2061-2090 average), and 2080s (2071-2100 average) under SSP3-7.0 scenarios. Panels (m-p) represent the annual mean concentrations of NO_3^- concentrations for 2030s (2021-2050 average), 2050s (2041-2070 average), 2070s (2061-2090 average), and 2080s (2071-2100 average) under SSP5-8.5 scenarios.

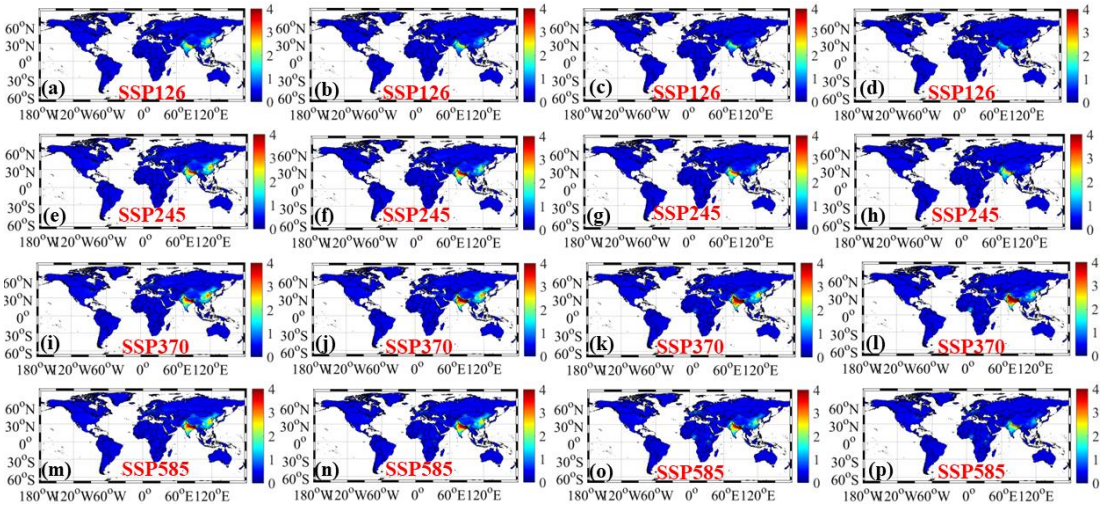

Figure S14 Spatial variations of projected global ambient HNO_3 concentrations under different climate change scenarios (Unit: μg N m^{-3}). Panels (a-d) represent the annual mean concentrations of HNO_3 concentrations for 2030s (2021-2050 average), 2050s (2041-2070 average), 2070s (2061-2090 average), and 2080s (2071-2100 average) under SSP1-2.6 scenarios. Panels (e-h) represent the annual mean concentrations of HNO_3 concentrations for 2030s (2021-2050 average), 2050s (2041-2070 average), 2070s (2061-2090 average), and 2080s (2071-2100 average) under SSP2-4.5 scenarios. Panels (i-l) represent the annual mean concentrations of HNO_3 concentrations for 2030s (2021-2050 average), 2050s (2041-2070 average), 2070s (2061-2090 average), and 2080s (2071-2100 average) under SSP3-7.0 scenarios. Panels (m-p) represent the annual mean concentrations of HNO_3 concentrations for 2030s (2021-2050 average), 2050s (2041-2070 average), 2070s (2061-2090 average), and 2080s (2071-2100 average) under SSP5-8.5 scenarios.

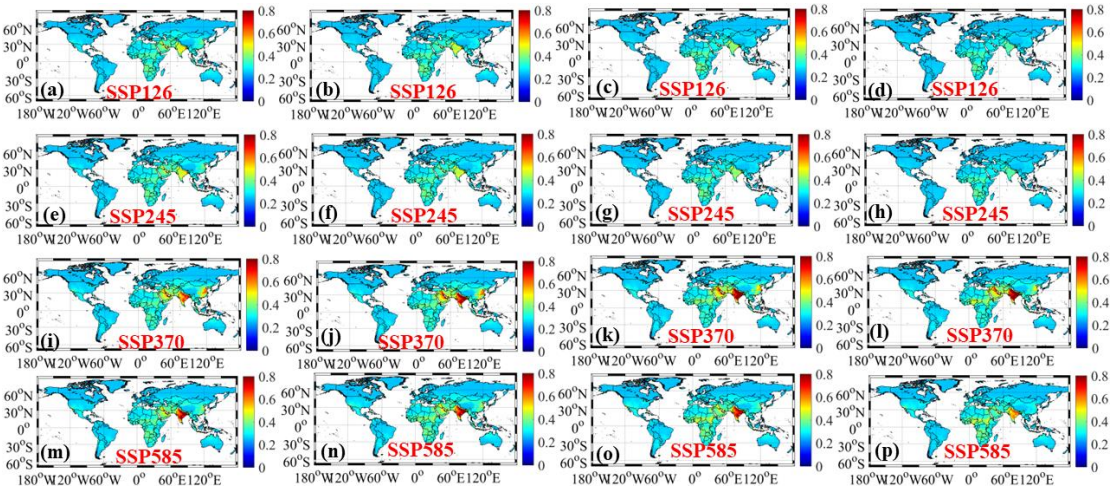

Figure S15 Spatial variations of projected global ambient NH_3 concentrations under different climate change scenarios (Unit: μg N m^{-3}). Panels (a-d) represent the annual mean concentrations of NH_3 concentrations for 2030s (2021-2050 average), 2050s (2041-2070 average), 2070s (2061-2090 average), and 2080s (2071-2100 average) under SSP1-2.6 scenarios. Panels (e-h) represent the annual mean concentrations of NH_3 concentrations for 2030s (2021-2050 average), 2050s (2041-2070 average), 2070s (2061-2090 average), and 2080s (2071-2100 average) under SSP2-4.5 scenarios. Panels (i-l) represent the annual mean concentrations of NH_3 concentrations for 2030s (2021-2050 average), 2050s (2041-2070 average), 2070s (2061-2090 average), and 2080s (2071-2100 average) under SSP3-7.0 scenarios. Panels (m-p) represent the annual mean concentrations of NH_3 concentrations for 2030s (2021-2050 average), 2050s (2041-2070 average), 2070s (2061-2090 average), and 2080s (2071-2100 average) under SSP5-8.5 scenarios.

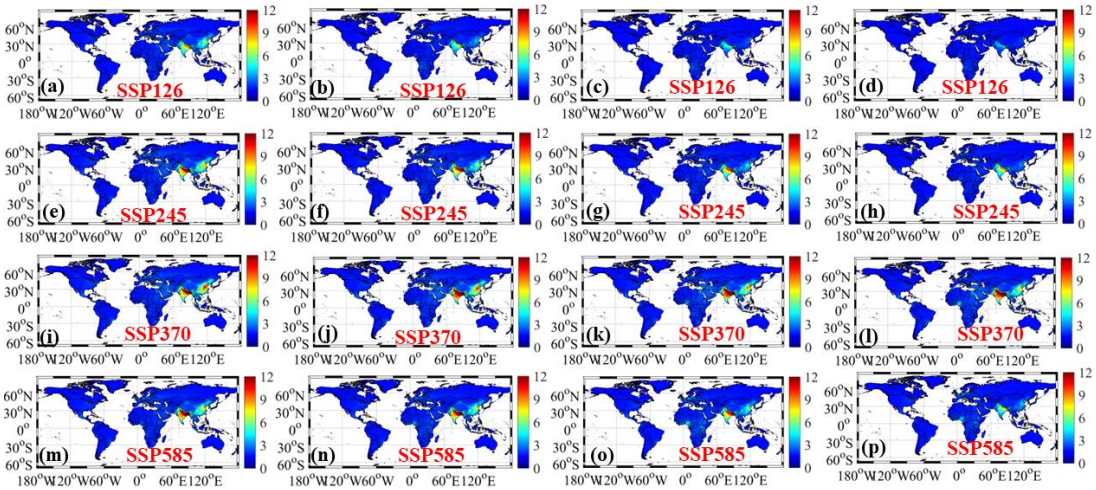

Figure S16 Spatial variations of projected global ambient NH_4^+ concentrations under different climate change scenarios (Unit: μg N m^{-3}). Panels (a-d) represent the annual mean concentrations of NH_4^+ concentrations for 2030s (2021-2050 average), 2050s (2041-2070 average), 2070s (2061-2090 average), and 2080s (2071-2100 average) under SSP1-2.6 scenarios. Panels (e-h) represent the annual mean concentrations of NH_4^+ concentrations for 2030s (2021-2050 average), 2050s (2041-2070 average), 2070s (2061-2090 average), and 2080s (2071-2100 average) under SSP2-4.5 scenarios. Panels (i-l) represent the annual mean concentrations of NH_4^+ concentrations for 2030s (2021-2050 average), 2050s (2041-2070 average), 2070s (2061-2090 average), and 2080s (2071-2100 average) under SSP3-7.0 scenarios. Panels (m-p) represent the annual mean concentrations of NH_4^+ concentrations for 2030s (2021-2050 average), 2050s (2041-2070 average), 2070s (2061-2090 average), and 2080s (2071-2100 average) under SSP5-8.5 scenarios.